# EXPERIMENTAL INVESTIGATION OF APPARENT SHALE PERMEABILITY WITH CONSIDERATION OF GAS SLIPPAGE AND STRESS-DEPENDENCE EFFECTS

Agustín Guillermo Garbino, ITBA/Texas Tech University, agustin.garbino@tecpetrol.com;
Matías Alejandro Urio, ITBA/Texas Tech University, mugr@chevron.com

**Palabras claves**

Shale Permeability, Stress Dependency, Flow regimes, Knudsen Number.

**Resumen**

Se realizaron mediciones de permeabilidad en muestras de rocas de shale gas correspondientes a la formación Eagle Ford, Texas, USA. Mediante el uso de un moderno permeabilímetro, cuyo funcionamiento se basa en el avance de un pulso de presión enviado a través del espacio poral del testigo, se busca entender la permeabilidad de este shale y su variación frente a diferentes presiones de confinamiento y presiones porales. El empleo de helio y metano como fluido de ensayo, en vez de líquidos, acortó el tiempo de cada medición y nos permitió analizar las diferencias debidas a los efectos de adsorción del gas y al "efecto támiz" de la fina estructura poral frente a moléculas de mayor tamaño como las presentes en el gas de reservorio. Además, las muestras fueron sometidas a una serie de mediciones en las cuales se mantuvo constante el estrés efectivo y se incrementó gradualmente la presión de confinamiento y la presión poral con el fin de cuantificar el aparente aumento de permeabilidad debido al efecto Klinkenberg. Nuestros resultados muestran que la habitual suposición de que el efecto de *gas slippage* puede ser despreciado a presiones mayores a 7 MPa no siempre es válida. A su vez, se aplican métodos recientes para identificar la desviación del flujo Darcy hacia regímenes de flujo difuso con el objetivo de obtener mediciones más precisas de la permeabilidad de la roca.

**Abstract**

Permeability measurements has been conducted on gas shale rocks from Eagle Ford plays. Using the newly developed pressure pulse decay permeabilimeter, AutoLab 1000, we try to understand permeability in this organic-rich gas shale and its sensitivity to different confining pressure and pore pressure. The use of helium and methane as pore fluid instead of liquids allowed as to make quick measurements and consider the differences due to gas adsorption and the molecular sieving effect of the fine pore structure to large molecules such as reservoir gases. Additionally, the samples were subjected to a series of measurements in which effective stress remains constant but increasing confining pressure and pore pressure step by step, in order to quantify the apparent increase of permeability due to Klinkenberg effect. Our results show that the common assumption that gas slippage can be neglected at pore pressure higher than 7 MPa is inaccurate. We also apply recent methods to identify deviation from Darcy to slip, transition and free molecular flow regimes to measure permeability more accurately.

## 1 - Introduction

The understanding and appropriate characterization of rock mechanical properties and petrophysics such as permeability has become crucial to have a successful shale development and production.

In this type of reservoirs heterogeneity from the basin-scale geology down to the nanometer-scale pore structure exist, resulting in multiple scales of porosity and permeability. Although complex natural and induced fractures may control the reservoir performance at early stages, it is the matrix properties that drive how a well will perform over longer periods of time. As intrinsic permeability evolves with time during production due to stress effects and flow regime effects it is necessary to quantify the sensitivity to these effects.

During shale gas production, as pore pressure is decreased, the matrix feels an increase in effective stress (difference between the confining pressure and pore pressure) which leads to lower permeabilities because of the pore throats narrowing. In contrast, flow regime impacts on permeability as well. In the shale gas literature, transport of gas through the rock matrix is described as a combination of Darcy´s flow and diffusion flow, especially at low gas pressures and/or porous rocks dominated by micropores (Cui *et al*., 2009; Heller *et al.*, 2014). While in Darcy´s flow continuum assumption is valid and flow rate is proportional to pressure gradient, in diffusion flow molecules move independently of one another and flow is driven by gas molecule-molecule collisions and gas molecule-pore wall collisions (figure 1). If there is a contribution of diffusion flow to the total flux, molecular transport exists along the walls of the flow channels. This effect, also known as Klinkenberg slip effect, manifest itself at low pore pressures as an apparent increase in the permeability of the rock. In this case, laboratory measurements need to be corrected for gas slippage in order to be used in reservoir models.

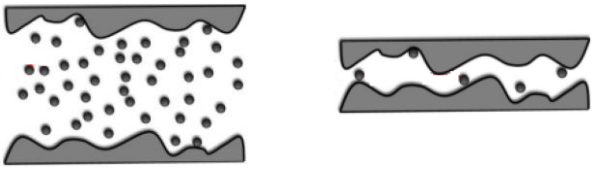

**Figure 1**. *Left*: Darcy´s flow. *Right:* Diffusion flow. (Modified from Nazari *et al.,* 2016).

According to the comprehensive study presented by Cui *et al.* (2009), both effects could be separated: the reduction of permeability with depletion and the increase in permeability associated with Knudsen diffusion and molecular slippage at very low pore pressure. Our study shows experimental results that gas slippage can have a significant effect on permeability for shale gas reservoir rocks, even when permeability measurements are made at high pore pressures (>7 Mpa), where gas slippage is assumed to be negligible by many researchers (Cui *et al.*, 2009; Heller *et al.*, 2014).

In this paper, we present experimental data of two intact samples that cover a wide range of permeabilities at different conditions. For comparison, each sample was measured with helium and methane as pore fluids. First, we focused on the stress-dependence of permeability by leaving confining pressure constant (15 MPa) and changing pore pressure from 1MPa to 12MPa. Then we quantify the Klinkenberg effect at a given constant effective stress increasing step by step the confining pressure and pore pressure. Finally, based on the results from above, we analyze qualitatively the impact on permeability due to adsorption effects.

## 2 – Methodology

### *Sample set up*

As stated before, permeability measurements were conducted on a shale rock sample from Eagle Ford formation.

To prepare the sample for the experiment, the contours of the top and bottom surfaces were limed using sandpaper until the surface was sufficiently smooth to prevent any flow leakage caused by superficial irregularities. The sample was then weighted, and their lengths and diameters were measured using a caliber.

To remove the initial water, the rock sample was dried at 105 °C overnight, while connected to the vacuum pump. All experiments were performed at constant temperature of 24 °C.

***Pulse decay technique***

The pressure pulse decay or unsteady state technique, shown schematically in Figure 2, consists of an upstream and downstream reservoir and a core holder. A small pressure pulse is applied from the upstream reservoir to the downstream reservoir, though the pore space of the sample, and the pressure changes in the two reservoirs are recorded as a function of time. By fitting the resulting pressure curves to a flow model, permeability of the rock sample can be determined.

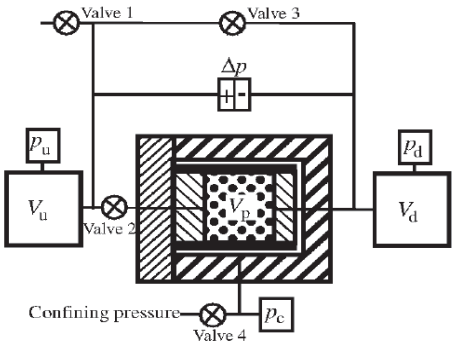


**Figure 2**. Schematic sketch of a pulse decay experimental apparatus (CUI *et al.*, 2009).

The experimental set up allows to apply confining pressure to represent reservoir stress conditions. The pore pressure is supplied from a gas bottle and its desired pressure for a test is regulated by a pressure regulator.

After setting the initial confining pressure, the initial pore pressure must also be set. In order to do this, valves 1, 2 and 3 are open, and gas is then injected into the whole system. The upstream pressure is regulated with a piston, and the system pressure is measured in both the downstream and upstream reservoirs using transducers. Once pressure stabilizes in the whole system, valves 2 and 3 are closed. Afterwards, pressure in the upstream reservoir is increased by a few percent (e.g. 5 %). Once it reaches equilibrium, valve 2 is open and a pressure pulse is sent from the upstream reservoir to the downstream reservoir, through the sample. The response from the downstream reservoir is measured. With the functions of *Pu(t)* and *Pd(t)* it is possible to calculate the dimensionless differential pressure ($\Delta P_D$), which is defined as follows:

$$\Delta P_D = \frac{P_u(t) - P_d(t)}{P_u(0) - P_d(0)} \quad \text{(1)}$$

The *ΔP versus t* data can then be analyzed to determine the sample permeability based on an analytical solution describing the pressure changes during the experiment with known parameters of reservoir volumes, sample pore volume and gas properties (Cui *et al.*, 2009).

If the pressure changes in the upstream reservoir are small (i.e. < 5%), then the experimental differential pressure at larger times becomes a single exponential function of time and can be approximated as (Suntherland and Cave, 1980):

$$\Delta P(t) = \Delta P_0 \, e^{-mt} \quad \text{(2)}$$

Where $\Delta P_0$ is the pressure pulse applied and $m$ depends on the permeability as follows:

$$m = -\frac{k\left(\frac{A}{L}\right)\left(\frac{1}{V_u}+\frac{1}{V_d}\right)}{\mu\beta} \quad \text{(3)}$$

Where:

$Vu$, $Vd$ are upstream and downstream reservoir volumes
$L$ = length of the sample
$A$ = cross-sectional area of the sample
$\mu$ = gas viscosity at temperature and mean pore pressure (Lemmon and Jacobsen, 2004)
$k$ = permeability of the sample
$\beta$ = gas compressibility

To calculate the permeability by the pulse decay technique it is then necessary to plot $\Delta P_D$ logarithmically versus time, and approximate the curve for late time data to the straight line which best fits. With the slope of the curve $m$ it is possible to calculate permeability with manipulation of Eqn 3, resulting in:

$$k = -\frac{m\left(\frac{L}{A}\right)\mu\beta(V_u V_d)}{(V_u+V_d)} \quad \text{(4)}$$

A model presented by (Cui *et al*. 2009) suggest than an adsorption factor $f_1$ may be added to the previous equation, which is dependent of the adsorption volume compared to the sample porosity. Since the measurements in this work where done with the Autolab1000 as the pulse decay apparatus, which does not contemplate adsorption for its permeability calculations, this factor was neglected. However, adsorption was taken into consideration for the analysis of apparent permeability when tested for different gases.

To analyze the impact of pore pressure in permeability several tests were conducted leaving the confining pressure constant, and only variating the pore pressure. Pulse decay tests were done with a confining pressure of 15 MPa and pore pressure ranging between 1 MPa and 12 MPa. Additionally, to consider slippage effects on permeability, a series of measurements were conducted at a constant effective stress of 10 MPa by increasing step by step pore pressure and confining pressure from 1 MPa to 12 MPa and from 11 MPa to 22 MPa respectively.

### *Klinkenberg effect*

Since the permeability tests were run using gas as pore fluid, Klinkenberg effect was considered. Due to gas molecule slippage in pore walls, the measured permeabilities using this kind of fluid are higher than the ones obtained using a liquid, and since permeability is defined as a physical property of porous rocks and thus independent of the fluid used, this must be corrected. It was necessary to run tests variating both confining pressure and pore pressure. The purpose was to obtain measurements of permeability with different pore pressure but keeping the effective stress constant. Once the data is obtained, permeability can be plotted versus the inverse of the average pore pressure (calculated from the average of the upstream and downstream pressures), as is indicated in the following equation derived by Klinkenberg (1941):

$$k_g = k_l\left(1+\frac{b}{p}\right) \quad \text{(5)}$$

where $k_g$ is the permeability measured with gas, $k_l$ is the permeability at infinite pressure (liquid or intrinsic permeability) and *b* is the slip factor.

Theory predicts a linear trend, from which the intrinsic permeability of the sample and Klinkenberg slip factor (b) can be calculated.

### *Adsorption*

As discussed by previous studies (Pang *et al.*, 2017; Cui *et al.*, 2009), adsorption effects have to be considered in experiments to determine permeability; otherwise permeability will be underestimated, especially for strongly adsorptive rocks such as organic-rich gas shales with high surface areas.

As commented before, although many models have been developed to measure permeability with considerations for gas adsorption, in this study two sets of tests were run for each sample using gases with different adsorption potentials for comparison. The first set was done using methane as a fluid, while the second was done using helium. The reason for this was to detect the differences in permeability measurements if two gases with different molecule size were used. As permeability for shales is ultra low, adsorptive effects must be taken into consideration when measuring permeability. Considering that shales take the role of source rocks in the oil and gas generation process, these rocks are usually strongly adsorptive to hydrocarbon gases such as methane.

## 3 - Results and Discussion

The Autolab1000 developed by New England Research Inc. was used as the pulse decay apparatus. It has the advantage of calculating permeability by its own, at different pulse frequencies. After measuring permeability of a sample from Eagle Ford with several pore pressures, the pressure versus time data results were analyzed to minimize potential errors in the data-matching approach. The permeability measurements that did not seem reliable were discarded. As shown in Figure 3, the *quality-check* criteria to arrive at a final permeability estimate was that if the calculated curve for downstream pressure (black curve) was smooth and matched the downstream pressure measured curve (blue curve), then the value was accepted, otherwise the measured value was rejected and not considered for the following analysis. The reference downstream pressure (pink curve) was also taken into consideration, since if this curve remained flat it means that frequency was not properly tuned.

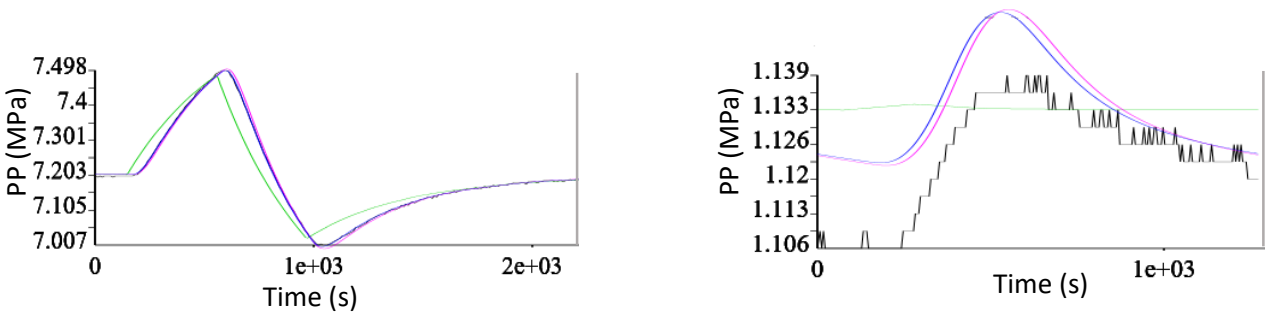


**Figure 3.** *Quality-check criteria*. The calculated curve (black curve) should match the measured curve (blue curve). Left: accepted analysis. Right: rejected analysis.

## Eagle Ford

### *1- Stress-dependent permeability*

The measured permeability, for both helium and methane, are plotted versus pressure in Figure 4.

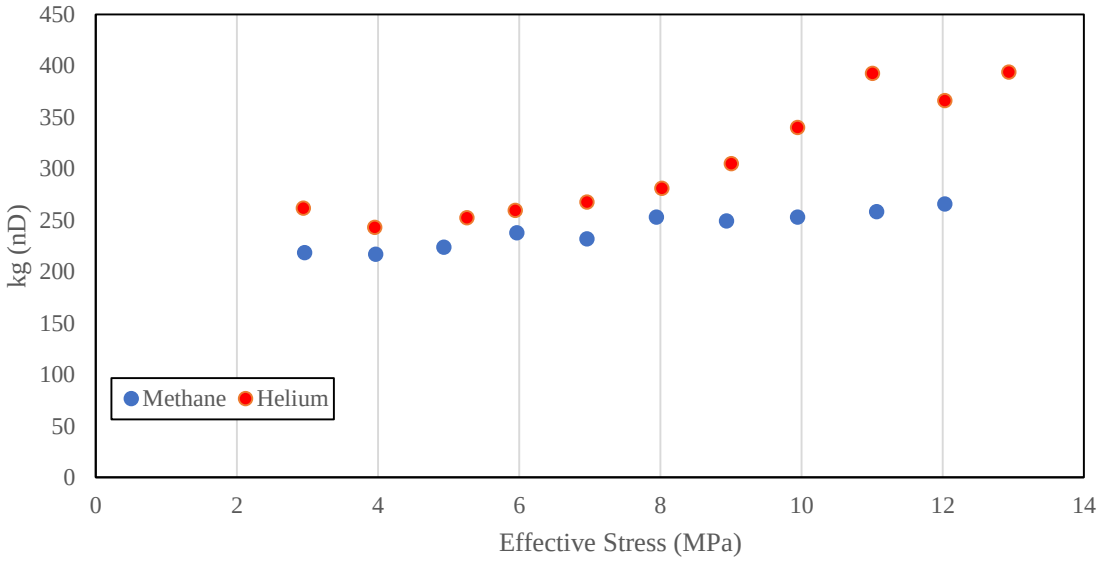


**Figure 4.** Permeability versus simple effective stress (CP – PP).

As shown in this figure, the measured permeability has an increasing trend, which is opposite to the behavior expected before running the test. As commented before, a decrease in pore pressure brings as consequence high competition between two opposite effects: pore narrowing because of increased effective stress which means a decrease in permeability; and slippage effect which causes an increase in the apparent permeability. However, this sample shows a strong slippage effect even at high pore pressures (low effective stresses).

Many researchers suggest that permeability measurements at high pore pressure (>7 MPa) are enough to obviate slippage effect in order to separate both effects. This assumption is not accurate in this case, so it is impossible to derive a permeability effective stress law and analyze the stress-dependency for this Eagle Ford sample.

Additionally, given that a clear tendency of effective stress effect could not be determined, we suppose that the compressibility of the rock is so low that yields in poor deformation when affected by stresses.

The difference between permeability values for methane and helium are attributed to adsorption effects and molecular sieving effect of the fine pore structure. As expected, the permeability values for methane are smaller than the ones for helium. The reason is that methane has bigger molecules than helium and is strongly adsorptive to shale rocks.

The relative error for low effective stresses goes from 11% to 17%, while for high effective stresses (low pore pressure) it ranges between 27% and 34%. This difference can be explained by the increasing slippage effect. At low pore pressure, the mean free path (distance between molecular collisions) increases significantly for both gases, this leads to more frequent molecules-pore walls collisions and thus Knudsen diffusion and molecular slippage increases. The apparent enhancement on permeability using helium relies on the strongest slippage effect on this gas because of its bigger mean free path ($\lambda_{He} \approx 2\lambda_{CH4}$).

### *2 - Klinkenberg effect*

Klinkenberg effect was analyzed by plotting the permeability measurements for constant effective stress versus the inverse of the average pore pressure. The results are presented in Figure 5.

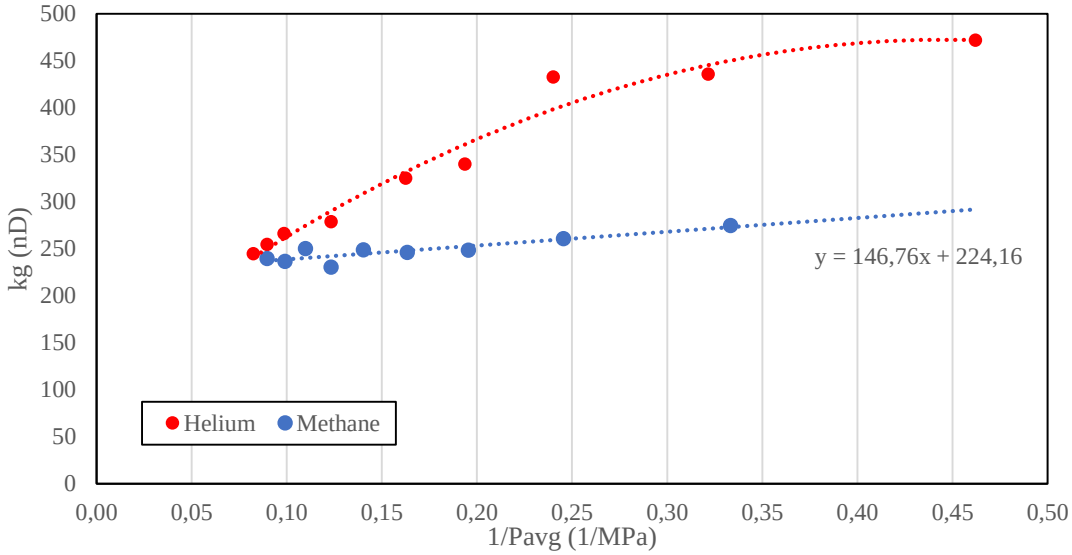


**Figure 5**. Klinkenberg plot. Note the deviation from a straight-line at low pore pressure for helium measurements.

As shown in this figure, the measured permeability with methane as pore fluid align in a straight line and it was possible to find a linear regression which represented appropriately the tendency of the points. Intrinsic permeability was obtained by a linear extrapolation. With the slope of the curve the slip factor was also calculated using Eqn. 5. However, a different behavior is observed for the measured data with helium as values start to deviate from a straight line at lower pore pressures.

**Table 1. Results for the intrinsic permeability and slip factor for methane measurements.**

| Symbol | Value |
|---|---|
| ***kl* (nD)** | 224.2 |
| ***b* (MPa)** | 0.65 |

### *2.1 – Flow regime characterization*

In order to find a reason for helium deviation from Klinkenberg´s linear behavior, Knudsen number was calculated for each experiment to verify the flow regime. Knudsen number is defined as:

$$Kn = \frac{\lambda}{D} \quad \text{..... (6)}$$

where $\lambda$ is the mean free path and $D$ is the conduit characteristic length. Based on $Kn$ it is possible to classify flow regimes in the system which characterize gas dynamics resultant from molecule-wall collisions (Zhang W-M *et al*., 2012):

I. For Kn < $10^{-2}$, flow is in the full continuum regime, the Darcy's law is valid.
II. For $10^{-2}$ < Kn < $10^{-1}$, flow can be considered as the slip flow. Slippage affect the flow, but continuum assumption is valid.
III. For $10^{-1}$ < Kn < 10, flow is in the transition region between slip and free molecule flow.
IV. For Kn > 10, the free-molecular regime. The collisions between the gas molecules and wall surfaces are dominant, and the intermolecular collisions can be ignored.

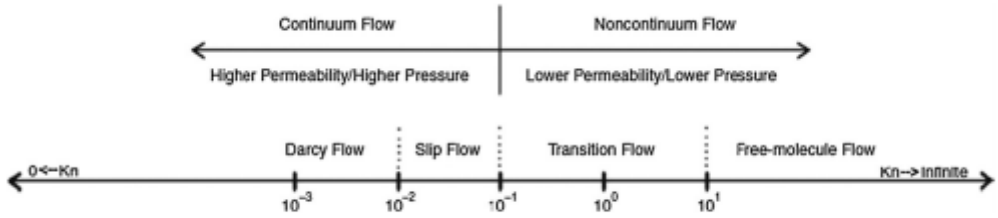


**Figure 6**: Flow regime categorized by Knudsen number (modified from Moghadam *et al.*, 2016).

For this purpose, a mercury injection test was performed using Quantachrome Poremaster 33 to characterize pore distribution, and calculate the mean pore size for the Eagle Ford sample to use it as the conduit characteristic length (Sakhaee-Pour et al. 2012).

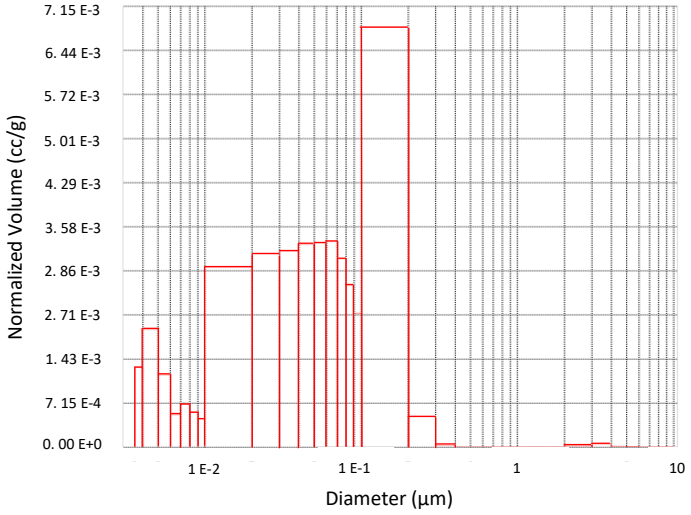


**Figure 7.** Normalized volume versus pore throat diameter. Note that a well-known probability function could not be fitted properly to this pore distribution.

The mean calculated for the pore distribution was 52 nm. However, as the mean pore size calculated appeared to be too big considering the low permeability of the sample if compared to other experiences from Nazari *et al.* (2016) and Pang *et al.* (2017), and as the mercury injection test did not provide reliable results (Figure 7), it was thought to be at least one order of magnitude lower. Further analysis was conducted for the mean free path, as it was estimated following a modified approach from Heller *et al.* 2013 (see Appendix 1). By considering the intrinsic permeability calculated previously, the result for the slit width was 1.4 nm.

Considering the overestimation of the mean pore size calculated by the mercury injection test and the uncertainties of the theoretical slit width approximation, a value for the conduit characteristic length ($D$) of 5 nm is used for the Knudsen number calculations, as it is believed to best represent the possible range of values from the expected order of magnitude. This value is also the lowest included in the pore-throat sizes range reported for source rocks from United States by Nelson (2009).

The gas mean free path was calculated based on the following equation:

$$\lambda = \frac{k_B T}{\sqrt{2}\pi\sigma^2 P} \quad \text{..... (7)}$$

where $k_B$ is the Boltzmann constant (1.3805 x$10^{-23}$ J/K), $T$ is the absolute temperature, $P$ is the gas pressure and $\sigma$ is the collision dimeter of gas molecule. Collision diameter can be estimated from gas viscosity using the following equation (Hildebrand, 1976):

$$\sigma^2 = \frac{2\sqrt{mk_BT}}{3\pi^{3/2}\mu} \quad \text{..... (8)}$$

where $m$ is the molecule mass and $\mu$ is the gas viscosity. All fluid parameters were extracted from the NSIT data base.

As shown in Figure 8 and Figure 9, the results for *Kn* were plotted versus permeability for both helium and methane, alongside with pressure versus permeability to show both trends together.

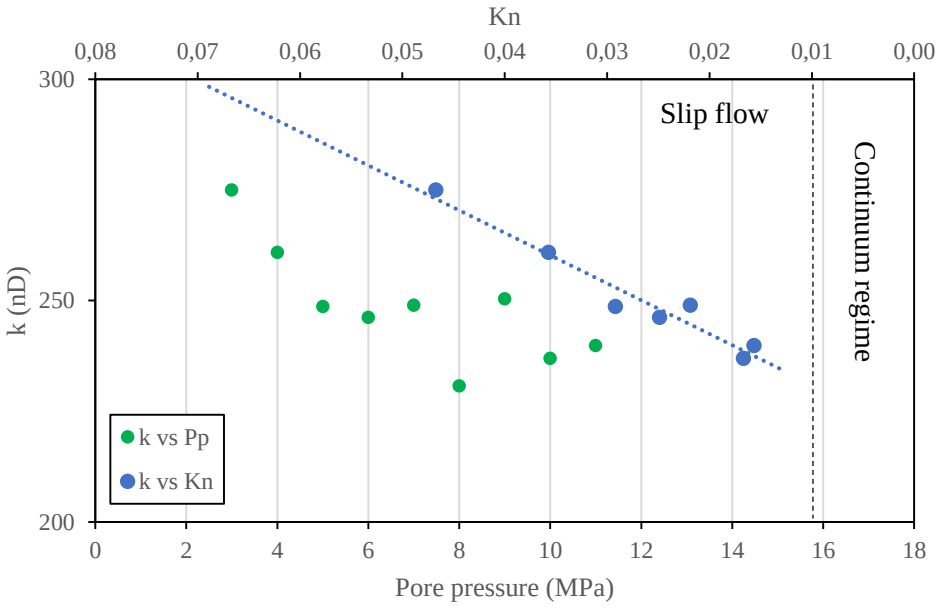


**Figure 8.** Measured permeability with methane versus Knudsen number and pore pressure. Note that Knudsen number results for methane align in a straight line.

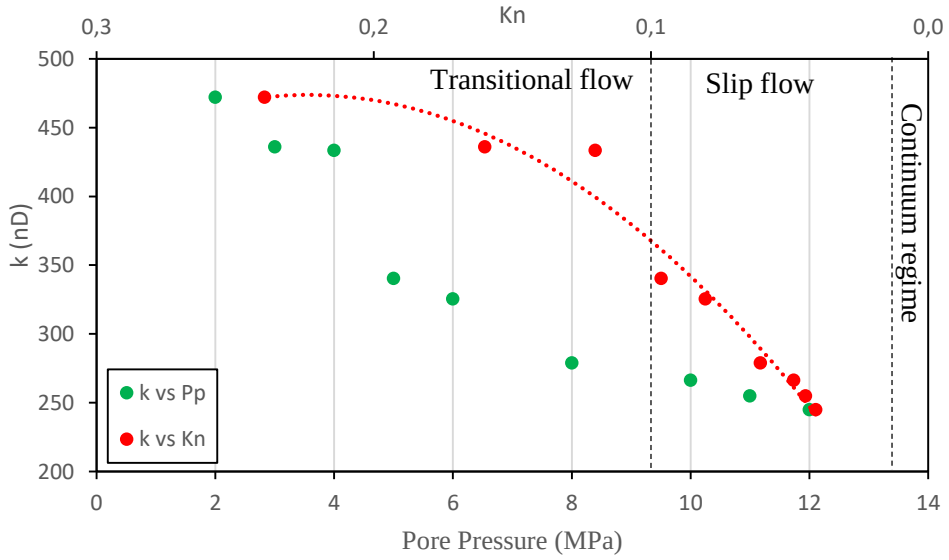

**Figure 9.** Measured permeability with helium versus Knudsen number and pore pressure. Note that Knudsen number results for helium do not align in a straight line.

The permeability measurements versus Knudsen number for methane lie close to a straight line. But for the measured permeability with helium, as the Knudsen number increases, the permeability does not follow a linear relationship, which means that Klinkenberg effect does not work in these regions. For higher pressures, *Kn* shows that the slip flow regime is predominant, while for lower pressures the transitional flow appears. We conclude that transitional flow regime is the reason for the linear trend deviation, opposite to Klinkenberg theory.

According to Beskok and Karniadakis (1999) higher order slip models should be used to predict the flow behaviour specifically when $Kn > 0.1$. Another approach, as shown by Nazari *et al.* 2016, is to use Klinkenberg approximation only where the slip-flow regime was predominant, based on the Knudsen number calculations.

As it has been stated before, the intrinsic permeability for helium measurements was calculated by a linear extrapolation, considering only high Knudsen numbers as shown is shown in Figure 10.

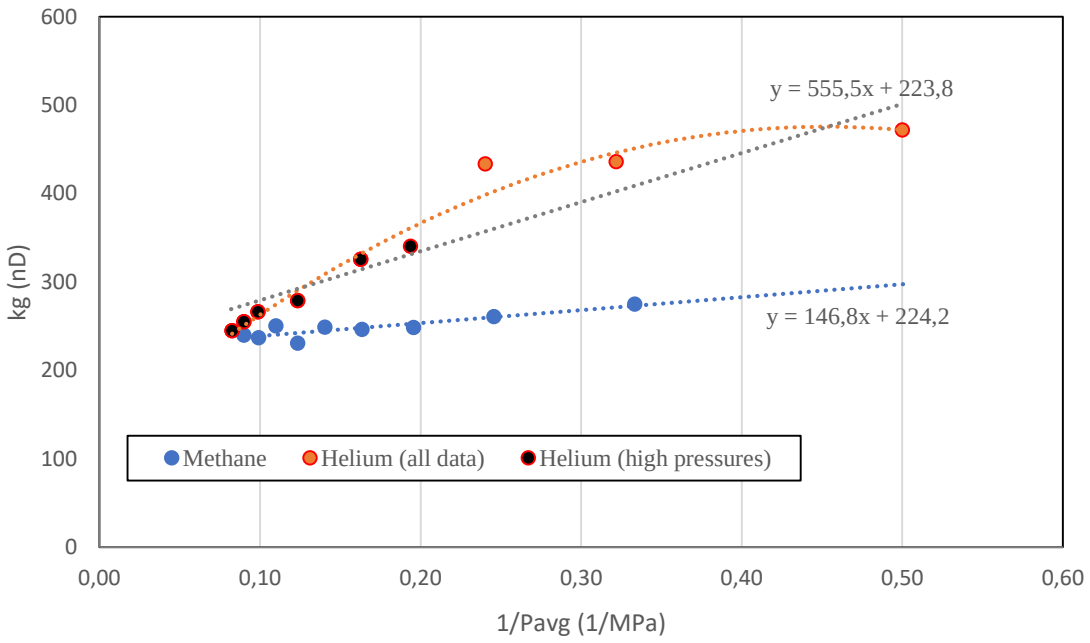


**Figure 10.** Klinkenberg plot. For helium, only permeabilities measured at high pore pressure were considered for extrapolation to estimate intrinsic permeability.

The result for the intrinsic permeability determined with helium is shown on Table 2. It may be noticed that the value almost does not differ from the calculated with methane. This is the expected behavior, since the intrinsic permeability is a property of the rock and does not depend on the fluid.

| **Table 2 - Results for intrinsic permeability and slip factor** | | |
|---|---|---|
| Symbol | Methane | Helium |
| ***kl* (nD)** | 224.2 | 223.8 |
| ***b* (MPa)** | 0.65 | 2.5 |

As commented below, even though high pore pressures are used, gas permeabilities obtained should be corrected for Klinkenberg gas slippage. This sample shows that, using helium as pore fluid, *kg* obtained would be 40%-20% higher than the intrinsic permeability at a mean pore pressure of 8 and 12 MPa respectively. For methane, *kg* shows to be 20-7% higher than *kl* at a pore pressure of 3 and 11 MPa respectively.

## 4 – Conclusions and Recommendations

In this paper, we conducted laboratory experiments on gas shales samples examining the effects of confining stress, pore pressure and pore fluid type on permeability. The main conclusions for this experimental study are the following:

- Our results show that the commonly used assumption that gas slippage can be neglected at pore pressure higher than 7 MPa is not always accurate. As shown on Eagle Ford sample, these high pressures do not guarantee that the Klinkenberg effect has no impact. The measurements were so affected by this that a tendency of effective stress effect could not be determined.
- As expected, the lower the pore pressure at a constant effective stress, the greater the impact of slippage in the measured permeability. The permeability of the rock is significantly enhanced at low pore pressures due to slippage effects.
- The best model for correcting permeability due to slippage depends on the predominant flow regime, which may be diagnosed by calculation of the Knudsen number. For methane, the straight-line trend of measured permeability versus the inverse of pore pressure and the results for the Knudsen number showed a predominance of the slip-flow regime for all the measured pore pressures, which validates even more the use of the Klinkenberg equation to calculate the intrinsic permeability. While for helium measurements, the transition from slip to transitional flow regime yields in a deviation from Klinkenberg straight-line trend. So, Klinkenberg model should only be applied when the slip-flow is present.
- For methane, lower pressures are required to enter the transitional flow than when using helium.
- The strong presence of a slip-dominant flow evidenced by the Knudsen number is also useful to justify the behavior shown by the permeability results, which is concluded to be strongly affected by slippage.
- Adsorption and molecular sieving effect of the fine pore structure also contributes to the difference between permeability values for methane and helium. As expected, the permeability values for methane are smaller than the ones for helium. The reason for this is that methane has bigger molecules than helium and is strongly adsorptive to shale rocks.
- For future works, we recommend measurements of the rock pore compressibility to validate if this is a possible cause for the anomalous behavior of the Eagle Ford sample. We also suggest measurements and calculation of the adsorption factor for an accurate value of permeability. Furthermore, the use of more accurate technologies to measure pore-throat sizes distribution is recommended as well for better flow regime characterization.

## APPENDIX 1

Assuming that the total flow is the sum of the viscous flow plus empirical constants times the Knudsen flow, assuming Darcy's law is valid to characterize the flow behavior, Heller et al. 2013 propose the following equation to calculate analytically the slit width (average pore diameter). This

is the result of combining Poiseuille equation for a viscous flow assuming slit-shaped pore geometry, with Darcy's law:

$$k = \underbrace{\frac{w^4}{12A}}_{k_l}\left[1 + \frac{1}{P}\underbrace{\frac{16c\mu}{w}\left(\frac{2RT}{\pi M}\right)^{1/2}}_{b}\right] \quad \text{.....(9)}$$

where c is an empirical constant, w is the slit width, A is the slit area, R is the gas constant, M is the molar mass of the gas, T is the temperature and μ is the gas viscosity.

Eqn 9 has the same form as the Klinkenberg's equation (Eqn 5). Consequently, in Heller *et al.* (2013) it is suggested to equal the slippage factor with the term multiplying *1/P* in order to calculate the slit width. However, a different approach was followed in this work with the purpose of calculating *w* without having to use any empirical constant.

First, the pore-throat area was rewritten as follows:

$$A = \frac{\pi w^2}{4} \quad \text{..... (10)}$$

Following Klinkenberg's model, replacing the term for the area in Eqn 9 by Eqn 10, after some manipulation the intrinsic permeability follows the following relation with the slit width:

$$k_l = \frac{w^2}{3\pi} \quad \text{..... (11)}$$

Eqn 11 can be reformulated to calculate the slit width:

$$w = \sqrt{3\pi k_l} \quad \text{..... (12)}$$

## Acknowledgements

This research was supported by the Petroleum Department from Texas Tech University. We thank Dr. James Sheng and Yu Pang, whose assistance, advice and constructive comments were essential for the development of this work.

## References

1. Heller R, Vermylen J, Zoback M: Experimental Investigation of matrix permeability of gas shales. *The American Association of Petroleum Geologists Bulletin*; v. 98; no. 5 (2014); 975–995.
2. Nazari Moghaddam R, Jamiolahmady M.: Slip flow in porous media. *Fuel 173* (2016); 298–310.
3. Zhang WM, Meng G, Wei X: A review on slip models for gas microflows. *Microfluid Nanofluid* (2012); 13:845–82.
4. Sakhaee-Pour A, Bryant S: Gas permeability of shale. *Society of Petroleum Engineers Reservoir Evaluation and Engineering* 2012; 15(04):401–9.
5. Hildebrand J: Viscosity of dilute gases and vapors. Proc Natl Acad Sci 1976; 73:4302–3.
6. NIST, National Institute of Standards and Technology. <http://webbook. nist.gov/chemistry/fluid/>; 2015.
7. Beskok A, Karniadakis GE: A model for flows in channels, pipes, and ducts at micro and nano scales. *Microscale Thermophys Eng* (1999); 3:43–77.

8. Moghadam A, Chalaturnyk R: Analytical and Experimental Investigations of Gas-Flow Regimes in Shales Considering the Influence of Mean Effective Stress. *April 2016 SPE Journal*

9. Pang Y, Soliman MY, Deng H, Xie X: Experimental and analytical investigation of adsorption effects on shale gas transport in organic nanopores. *Fuel 199* (2017); 272–288.

10. Nelson PH: Pore-throat sizes in sandstones, tight sandstones, and shales. *The American Association of Petroleum Geologists Bulletin*; v. 93, no. 3 (2009); 329– 340.

11. Cui X, Bustin AMM, Bustin RM: Measurements of gas permeability and diffusivity of tight reservoir rocks: different approaches and their applications. *Geofluids* (2009) 9; 208-223.

12. Jones SC: A technique for faster pulse-decay permeability measurements in tight rocks. *Society of Petroleum Engineers Reservoir Evaluation and Engineering* (1997); 12; 19-25.

13. Sutherland HJ, Cave SP: Argon gas permeability of New Mexico rock salt under hydrostatic compression. *Int. J. Rock Mech. Min. Sci. and Geomech.* (1980); Abstr.17; 281-288.

14. Lemmon EW, Jacobsen RT: Viscosity and Thermal Conductivity Equations for Nitrogen, Oxygen, Argon, and Air. *International Journal of Thermophysics* (2004); 25; 21-69.

15. Klinkenberg L.J: The permeability of porous media to liquids and gases. *In Drilling and Production Practice, American Petroleum Institute* (1941); 200-213.

## Brief Resume

**Agustin G. Garbino**, Ingeniero en Petróleo del Instituto Tecnológico de Buenos Aires recibido con honores. Actualmente desempeñándose como Ingeniero de Reservorios en Tecpetrol. Partícipe del Programa Research Experience for Undergraduate Students en Texas Tech University (Lubbock, TX, USA).

**Matías A. Urio**, Ingeniero en Petróleo del Instituto Tecnológico de Buenos Aires recibido con honores. Actualmente desempeñándose como Ingeniero de Producción en Chevron Argentina. Partícipe del Programa Research Experience for Undergraduate Students en Texas Tech University (Lubbock, TX, USA).